DOI: 10.1002/ejoc.200700294

Probing Receptor–Anion Interactions by Ratiometric Chemosensors Containing Pyrrolecarboxamide Interacting Sites

Chun-Lin Chen,[a] Tzu-Pin Lin,[a] Yen-Shiu Chen,[a] and Shih-Sheng Sun*[a]

Keywords: Receptors / Fluorescent probes / Molecular recognition / Anions

We have designed and synthesized a series of molecular probes integrating both an amide and a pyrrole functionality for anion-recognition and -sensing. The interactions between these probe molecules and various anions have been investigated to elucidate the influence of electronic effects on the anion-recognition site. Changes in the UV/Vis and fluorescence spectra in the presence of anions reveal that probes **1**–**5** typically display a strong response to cyanide. Moreover, the appearance of the ratiometric phenomenon upon interaction with anions further enhances spectral differentiation for anion-sensing. The mechanism for the reaction between the probe molecules and the anions has been further explored by ^{1}H NMR titration experiments. Anions strongly interacting with probes and producing large changes in the UV/Vis and fluorescence spectra during the titration usually result in deprotonation of the amide group, whereas weakly interacting anions initially form hydrogen bonds with amide and pyrrole NH groups followed by deprotonation at higher anion concentrations. The weakest anions, however, form only two or four hydrogen bonds with the amide and pyrrole N–H groups during the titrations. Moreover, both probes **2** and **3** are able to recognize cyanide in a semi-aqueous environment with extremely high selectivity. The formation of covalently bonded cyanohydrin derivatives from cyanide addition to an electron-deficient amide carbonyl center is attributed to the effectiveness of probes **2** and **3** in a semi-aqueous environment.

(© Wiley-VCH Verlag GmbH & Co. KGaA, 69451 Weinheim, Germany, 2007)

Introduction

In view of the critical roles played by anionic species in chemical, biological, and environmental processes, the molecular recognition of anions by synthetic chemosensors has been an active research area. Numerous efforts have been devoted to the development of abiotic receptors for anionic species.[1] Among the various artificial receptors reported in the literature, those employing polarized NH groups as anion-binding motifs have attracted considerable attention recently.[2] Notable examples include receptors containing pyrrolic moieties,[3] amide groups,[4] indolocarbazoles,[5] imidazolium groups,[6] and urea or thiourea derivatives.[7] Typically, the anions form N–H···A$^-$ hydrogen bonds with these receptors. However, it is not easy to clearly differentiate or predict whether the receptor–anion interaction is dominated by the formation of hydrogen bonding or anion-induced deprotonation in some cases, especially for acyclic receptors which usually lack complementary structures to accommodate the shape and/or size of the anions.[1c,8] The ability to establish hydrogen bonds between the anion and NH group is usually determined by the degree of electron deficiency on the interacting hydrogen atom (or proton acidity) and the electronegativity of the anion (or anion basicity). In some extreme cases, neat proton transfer from polarized NH groups to the anion occurs and this phenomenon has been documented in the literature.[1c,3e,4b,4e,7b–7d,7f,9]

Among the various signal-reporting techniques for analyte–receptor interactions, colorimetric and ratiometric fluorescence sensing offer several advantages, including visual monitoring, precise detection without interference due to medium effects, and an enhanced dynamic range, over simple detection based on fluorescence quenching or enhancement.[10] The ratio of the emission intensities at two different wavelengths is sufficient to determine the analyte concentration independent of probe concentration or any instrument-related parameters. The design of colorimetric and ratiometric fluorescence chemosensors also provides the basis for the manipulation and engineering of various photophysical processes with the ultimate goal being the selective and sensitive signaling of targeted species. Although a number of colorimetric and fluorescence sensors for anions have been developed, only a few such ratiometric fluorescent probes have been reported for anion-sensing in recent years.[4e,11]

Recently, Cheng and co-workers reported a dipyrrole-2-carboxamide–phenylene compound that exhibits a weak binding affinity for F$^-$ in DMSO solution.[12] A later report by Gale and co-workers on the same compound showed a

[a] Institute of Chemistry, Academia Sinica,
115 Nankang, Taipei, Taiwan, Republic of China
E-mail: sssun@chem.sinica.edu.tw

Supporting information for this article is available on the WWW under http://www.eurjoc.org or from the author.

 © 2007 Wiley-VCH Verlag GmbH & Co. KGaA, Weinheim

similar weak binding affinity for OAc^-, $PhCO_2^-$, and $H_2PO_4^-$.[13] The lack of a chromophoric moiety in this compound has hindered the use of optical methods as the detection tool to probe the receptor–anion interaction. Our recent work on cyanide-sensing prompted us to further explore the interaction modes between different anions and these probe molecules.[14] The molecular design of our anion probes incorporates an anion-recognition pocket within a chromogenic/fluorogenic moiety. Depending on the degree of interaction between the anion and the recognition pocket, the electronic perturbation on the chromophore would alter the HOMO–LUMO gap and change the color of the solution, the fluorescence wavelength, and the fluorescence intensity. The anion-binding pocket we studied comprises dual amide and pyrrole functional groups which are well known for their ability to form N–H···A$^-$ hydrogen bonds with specific anions. We envision different receptor–anion interaction modes could occur by varying the electron deficiency of the NH groups in the recognition pocket.

Herein we describe a series of bis(pyrrolecarboxamide)-derived ratiometric probes with a tweezer-type cleft for anions. These receptors provide varied interaction modes for different anions stemming from different structures and different pK_a values of the hydrogen-bond donors and the anion-recognition events can be easily probed by spectroscopic techniques. The receptor–anion interaction and the mechanism of the colorimetric and ratiometric fluorescent responses are explored and rationalized by ^{1}H NMR titration experiments and semi-empirical ZINDO calculations.

Results

Molecular Design, Synthesis, and Structures of the Anion Probes

The synthesis and structures of probes **1**–**5** are shown in Scheme 1. They were prepared by condensation of pyrrole-2-carbonyl chloride with the corresponding aryldiamine in CH_2Cl_2 with a small amount of triethylamine present in solution. Typical yields were between 20 and 70%. The identities and structures of all five compounds were characterized by ^{1}H NMR spectroscopy, high-resolution mass spectrometry, and elemental analysis.

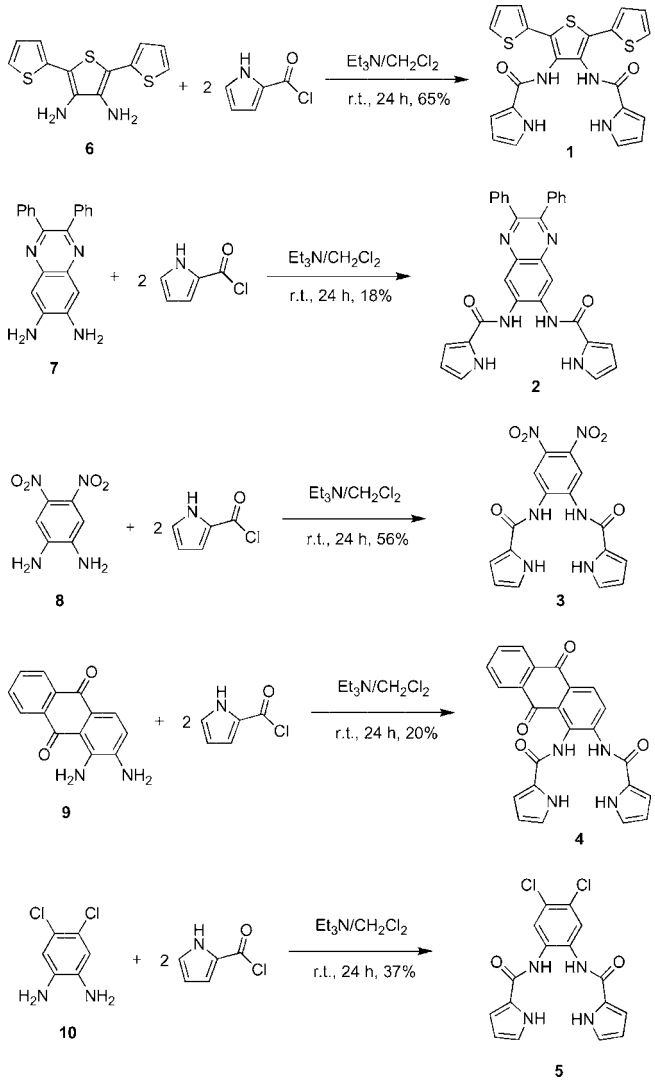

Scheme 1. Synthesis of probes **1**–**5**.

Table 1. Selective chemical shifts of probes **1**–**5** upon addition of 2 equiv. of anions in [D$_6$]DMSO solution.[a]

	δ [ppm]			
	Pyrrole N–H[b]	Amide N–H[b]	Phenyl C–H	Pyrrole C–H[c]
No anion	11.6 (**1**), 11.9 (**2**), 11.9 (**3**), 12.1 (**4**), 11.9 (**4**), 11.9 (**5**)	9.36 (**1**), 10.1 (**2**), 10.2 (**3**), 11.0 (**4**), 10.0 (**4**), 9.85 (**5**)	8.45 (**2**), 8.55 (**3**), 8.42 (**4**), 8.21 (**4**), 7.91 (**5**)	6.95 (**1**), 7.05 (**2**), 7.08 (**3**), 7.17 (**4**), 6.84 (**4**), 6.96 (**5**)
Cl^-	11.6 (**1**), 12.0 (**2**), 11.9 (**3**), 12.1 (**4**), 11.9 (**4**), 11.9 (**5**)	9.43 (**1**), 10.5 (**2**), 10.7 (**3**), 11.0 (**4**), 10.1 (**4**), 10.0 (**5**)	8.44 (**2**), 8.57 (**3**), 8.42 (**4**), 8.21 (**4**), 7.91 (**5**)	6.95 (**1**), 7.24 (**2**), 7.31 (**3**), 7.18 (**4**), 6.88 (**4**), 7.05 (**5**)
OH^-	b (**1**), b (**2**), b (**3**), b (**4**), b (**4**), b (**5**)	b (**1**), b (**2**), b (**3**), b (**4**), b (**4**), b (**5**)	8.85 (**2**), 8.68 (**3**), 8.33 (**4**), 8.14 (**4**), 8.37 (**5**)	6.70 (**1**), 6.77 (**2**), 6.59 (**3**), 6.84 (**4**), 6.64 (**4**), 6.61 (**5**)
$H_2PO_4^-$	12.8 (**1**), 12.8 (**2**), 11.9 (**3**), 12.7 (**4**), 12.8 (**5**)	11.0 (**1**), 11.3 (**2**), b (**3**), 11.2 (**4**), 11.0 (**4**), 11.2 (**5**)	8.43 (**2**), 8.80 (**3**), 8.32 (**4**), 8.14 (**4**), 7.84 (**5**)	6.77 (**1**), 6.96 (**2**), 6.86 (**3**), 6.99 (**4**), 6.91 (**4**), 6.90 (**5**)
OAc^-	12.0 (**1**), b (**2**), 11.6 (**3**), 12.4 (**4**), 12.6 (**5**)	10.8 (**1**), b (**2**), b (**3**), 11.2 (**4**), 11.1 (**5**)	8.67 (**2**), 8.88 (**3**), 8.34 (**4**), 8.15 (**4**), 7.96 (**5**)	6.84 (**1**), 6.92 (**2**), 6.74 (**3**), 7.03 (**4**), 6.93 (**4**), 6.96 (**5**)
F^-	b (**1**), b (**2**), b (**3**), b (**4**), 13.6 (**5**)	b (**1**), b (**2**), b (**3**), 12.7 (**4**), 12.3 (**5**)	8.90 (**2**), 8.95 (**3**), 8.62 (**4**), 8.11 (**4**), 8.50 (**5**)	6.70 (**1**), 6.91 (**2**), 6.79 (**3**), 6.95 (**4**), 6.97 (**5**)
CN^-	b (**1**), b (**2**), b (**3**), b (**4**), b (**5**)	b (**1**), b (**2**), b (**3**), b (**4**), b (**5**)	8.78 (**2**), 8.88 (**3**), 8.37 (**4**), 7.99 (**4**), 8.14 (**5**)	6.81 (**1**), 6.82 (**2**), 6.75 (**3**), 7.00 (**4**), 6.75 (**4**), 6.80 (**5**)

[a] The bold numbers in parentheses represent the probe codes. [b] The signal disappeared or was too broad to assign a position. [c] The proton at the 3-position of the pyrrole ring.

 © 2007 Wiley-VCH Verlag GmbH & Co. KGaA, Weinheim

Anion-Binding Monitored by ^{1}H NMR Titration in [D$_6$]DMSO Solution

In order to pinpoint the anion-receptor sites and fully explore the interaction modes between the anions and probe molecules, we carried out ^{1}H NMR titration experiments in [D$_6$]DMSO solution. It was anticipated that the ^{1}H NMR pattern would provide informative structural details after the anion–probe interaction and possibly define the interacting sites. Table 1 summarizes the selective chemical shifts of the probes upon addition of 2 equiv. of anions.

Titration of Cl$^-$ and H$_2$PO$_4^-$ against Probes 1–5

The ^{1}H NMR spectra of all five probes titrated against Cl$^-$ displayed a downfield shift of the amide NH proton signals and no or a very minor upfield shift of the aromatic proton signals indicating a weak hydrogen-bonding interaction between the chloride ion and amide NH protons. In the cases of probes **2**, **3**, and **5**, the signal of the pyrrole proton at the 3-position also displayed a noticeable downfield shift indicating a hydrogen-bonding interaction between the chloride ion and these C–H protons. This observation suggests that the pyrrole N–H groups adopt an *anti* conformation with respect to the amide N–H groups. Only one amide NH signal showed a downfield shift in probe **4** which is attributed to the steric repulsion between the anthraquinone oxygen atom at the 9-position and the amide carbonyl oxygen atom forcing a twisted conformation out of the anthraquinone plane. In general, the extent of the amide NH signal downfield shift decreases in the order **3** $>$ **2** $>$ **5** $>$ **4** $\approx$ **1**, which also implies that the electron deficiency of the corresponding amide NH group in these probe molecules follows the same order.

Unlike the cases observed with the chloride titrations, with $H_2PO_4^-$ all five probes studied here showed downfield shifts for both the amide and pyrrole N–H proton signals and upfield shifts of the aromatic proton signals during the titrations. This observation indicated a collective hydrogen-bonding interaction between the $H_2PO_4^-$ and all four amide and pyrrole N–H protons.

Titration of OH$^-$ against Probes 1–5

Addition of OH$^-$ to the probe solutions was expected to induce deprotonation of the acidic N–H groups and the patterns of the peak shifts in the ^{1}H NMR spectra could serve as an indication of the deprotonation process for other anion–probe interactions. The general features of the changes in the ^{1}H NMR spectra upon addition of OH$^-$ to the probe solution are (1) the disappearance of the deprotonated amide N–H signal, (2) a downfield shift of the neighboring phenyl proton peak of the amide N–H group at $\delta \approx 8$–9 ppm due to an electrostatic through-space effect,[15] (3) an upfield shift of the signal of the phenyl proton in position 3 of probe **4** indicating a deprotonation of the amide N–H group in position 1, which exerted a through-bond effect causing the upfield shift, (4) peak broadening (probes **2**, **4**, and **5**) or a shift to an upfield position (probe **3**) of the pyrrole N–H signal, and (5) upfield shifts of all the other aromatic protons signals.

On the other hand, the ^{1}H NMR spectra of probe **1** show that the amide and pyrrole N–H signals undergo a downfield shift on addition of the first equivalent of OH$^-$, as typically observed when a hydrogen-bonding interaction is established. Meanwhile, the peaks of the aromatic protons do not exhibit noticeable shifts but become broad. The amide N–H peak started to disappear and the peaks of aromatic protons displayed a significant upfield shift after the addition of more than 1 equiv. of OH$^-$. A similar feature also was observed with other probe molecules that are expected to undergo a neat proton transfer induced by basic anions.

Titration of OAc$^-$ against Probes 1–5

Titration of OAc$^-$ against [D$_6$]DMSO solutions of probes **1**, **4**, and **5** resulted in downfield shifts for both the amide and pyrrole NH peaks indicating a typical hydrogen-bonding interaction. The downfield shift of the amide N–H signal is apparently more significant than that of the pyrrole N–H signal in probes **1**, **4**, and **5**. Gale and co-workers have reported the crystal structure of the acetate complex of *N*,*N*′-(1,2-phenylene)bis(1*H*-pyrrole-2-carboxamide) in which the acetate is hydrogen-bonded to both amide N–H groups but to only one pyrrole N–H group.[13] We believe a similar binding mode also possibly exists in the associated acetate complexes of probes **1**, **4**, and **5** in solution.

On addition of less than 1 equiv. of OAc$^-$, the amide and pyrrole N–H signals of probe **2** become broad and shift slightly downfield, indicative of a dynamic process occurring at a rate comparable to the ^{1}H NMR spectroscopic timescale. The amide N–H peak gradually disappeared after initial addition of OAc$^-$. The quinoxaline CH proton signal shifted to a downfield position and the rest of the aromatic proton signals displayed upfield shifts. These observations suggest initial hydrogen-bonding formation between OAc$^-$ and possibly two amide N–H protons and one pyrrole N–H proton followed by an intramolecular proton transfer from one of the amide N–H protons to OAc$^-$ (see Scheme 2).

Figure 1 shows the ^{1}H NMR titration of a [D$_6$]DMSO solution of probe **3** with OAc$^-$. On addition of the first equivalent of OAc$^-$, all the pyrrole proton signals (N–H and C–H) shifted to an upfield position, while phenyl proton signal exhibited a downfield shift. The amide N–H proton signal did not shift but became broad and gradually disappeared. This phenomenon implies a neat proton transfer from an amide N–H proton to OAc$^-$. The spectra virtually did not change in the presence of 1–2 equiv. of OAc$^-$. The addition of more than 2 equiv. of OAc$^-$ resulted in a downfield shift of the pyrrole N–H proton signal and a slight upfield shift of the phenyl proton signal. This is an indication of a hydrogen-bonding interaction between the pyrrole N–H protons and OAc$^-$ after amide NH deprotonation. As shown later in Table 3, the association constant for the sec-

 © 2007 Wiley-VCH Verlag GmbH & Co. KGaA, Weinheim

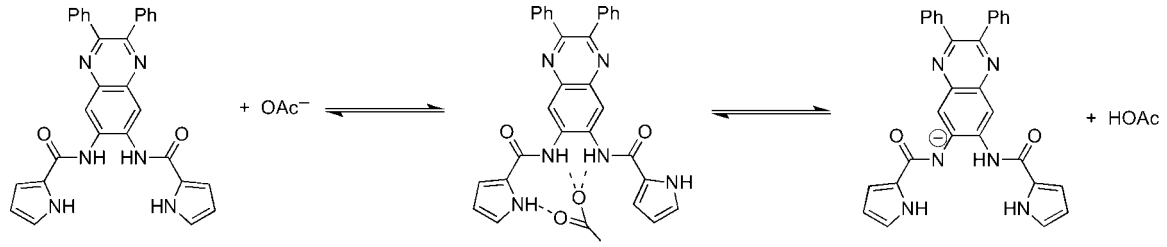

Scheme 2. Proposed stepwise equilibria formed between probe **2** and acetate.

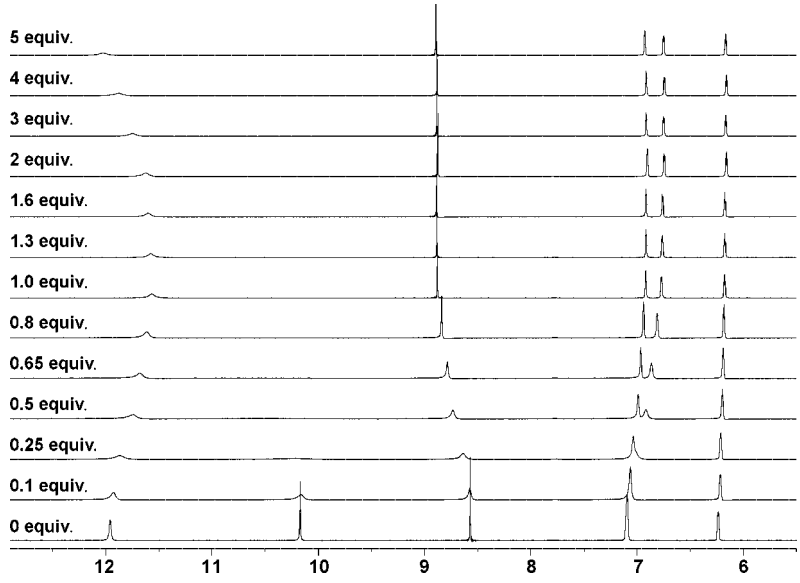

Figure 1. Plots of ^{1}H NMR spectra of probe **3** on addition of OAc^- in [D_6]DMSO.

ond step of Scheme 3 is about three orders of magnitude smaller than the proton dissociation constant for the first step which implies the existence of unfavorable electrostatic repulsion between the deprotonated form of **3** and the incoming acetate anion in the second equilibrium. Nevertheless, the distribution of negative charge over the entire dinitrobenzene region due to the strong electron-withdrawing nature of the nitro functionality and the favorable resonance effect would expect to overcome such electrostatic repulsion. To the best of our knowledge, this type of acidic

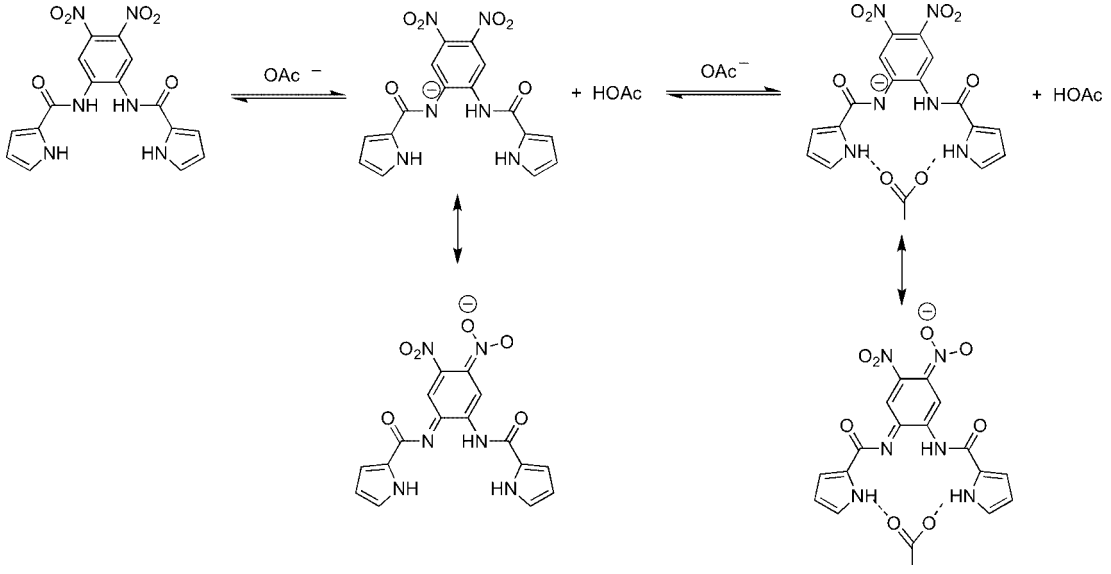

Scheme 3. Proposed stepwise equilibria between probe **3** and acetate.

 © 2007 Wiley-VCH Verlag GmbH & Co. KGaA, Weinheim

N–H NMR shift pattern is the first reported example of a neat proton transfer of the most acidic protons followed by the formation of hydrogen bonds to the less acidic protons.

Titration of F^- against Probes 1–5

The titration of F^- against a [D_6]DMSO solution of probe **1** resulted in a downfield shift and peak-broadening of both the amide and pyrrole N–H signals, which indicates a typical hydrogen-bonding interaction between F^- and the probe **1**. Similar hydrogen-bonding-induced downfield shifts were observed for both amide and pyrrole N–H proton signals on addition of the first equivalent of F^- to DMSO solutions of probes **2**–**5**. The amide N–H signals gradually disappeared on addition of 1–2 equiv. of F^-. Concomitantly, the terthiophene proton signals of **1**, the quinoxaline peak of **2**, and the phenyl peaks of **3**–**5** showed slight upfield shifts. This observation is consistent with a neat deprotonation of an amide N–H group to form the HF_2^- anion.[16] Representative ^{1}H NMR titration spectra of probe **3** in [D_6]DMSO in the presence of Bu_4NF are shown in Figure 2.

Titration of CN^- against Probes 1–5

Addition of CN^- to [D_6]DMSO solutions of probes **4** and **5** resulted in the rapid disappearance of NH proton signals of amide and pyrrole due to peak broadening. The downfield shift of the phenyl proton signal of probe **5** suggested deprotonation of the amide NH proton by CN^- owing to a through-space electrostatic interaction.[15] The doublet of the phenyl proton at $\delta \approx 8.2$ ppm of probe **4** experienced an upfield shift to ca. 8 ppm on addition of 5 equiv. of CN^- which implies deprotonation from the amide NH proton by CN^- to generate a shielding effect by through-bond propagation of negative charge onto the phenyl ring. The upfield shift of the thiophene proton signals of probe **1** also indicated an increase in the electron density of the aromatic rings due to deprotonation of the amide NH proton.

Formation of the cyanide adducts by interaction of probes **2** and **3** with CN^- was reported in our previous work.[14] Addition of CN^- to a [D_6]DMSO solution of probe **3** resulted in the slow disappearance of the amide NH proton signal, while the pyrrole NH peak shifted to an upfield position. The phenyl proton signals also exhibited a downfield shift due to the electrostatic through-space effect. The spectral shift virtually stops after addition of 2 equiv. of cyanide. Addition of trifluoroacetic acid turned the solution back to colorless. Scheme 4 outlines the proposed mechanism for the formation of the cyanohydrin derivative. The formation of the cyanide adduct was further confirmed by mass spectrometry and the ^{13}C NMR spectrum.[14] The electrospray ionization mass spectrum of the precipitated orange solid showed a molecular mass of 948.60 which corresponds to the formula [**11** + 2 Bu_4N^+ + CN^-]$^+$ (calcd. 948.68). The formation of the cyanide adduct is further indirectly supported by anion competition experiments. The yellowish color of the cyanide–probe **3** complex persists in the presence of a 50 equiv. excess of other anions except for $HP_2O_7^{3-}$, $H_2PO_4^-$, and HSO_4^-. The ability to protonate the cyanide adduct by these three anions and turn the solution color back to colorless is consistent with the final process depicted in Scheme 4.

Figure 3 shows the ^{1}H NMR spectra of **2** upon addition of tetrabutylammonium cyanide in [D_6]DMSO solution. The response of probe **2** to the addition of CN^- is similar to that of probe **3**. The most significant differences come from the gradual disappearance of the pyrrole NH proton signal and the downfield shift of the β proton signal of the pyrrole on addition of the cyanide anion. This observation confirms the interaction of pyrrole moieties with the cyanide anion in the probe–cyanide complex. The amide protons in **2** are expected to be less acidic than those in **3**.

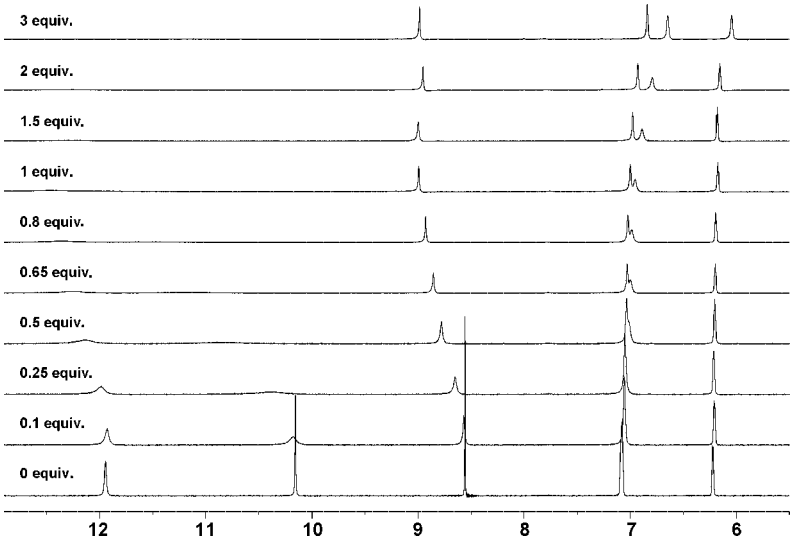

Figure 2. Plots of ^{1}H NMR spectra of probe **3** on addition of F^- in [D_6]DMSO.

 © 2007 Wiley-VCH Verlag GmbH & Co. KGaA, Weinheim

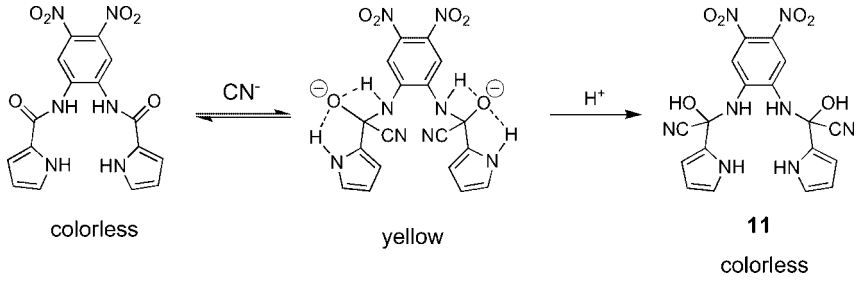

Scheme 4. Proposed cyanohydrin formation from reaction of probe **3** and cyanide.

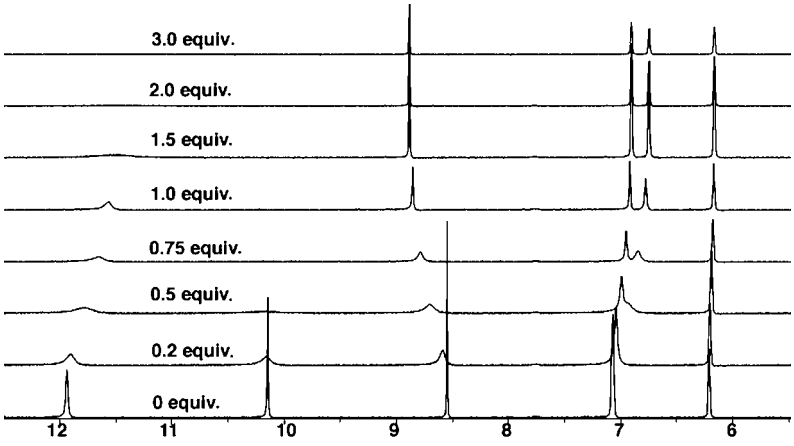

Figure 3. Plots of ^{1}H NMR spectra of probe **3** on addition of CN^- in [D_6]DMSO.

Thus, the proton exchange is expected to involve not only the amide protons but also possibly the pyrrole NH protons as well.

Photophysical Properties and Colorimetric and Fluorescence Anion-Sensing in CH_3CN Solution

Table 2 collects the photophysical data for probes **1**–**5** in CH_3CN solution. Probes **1**–**5** all exhibit a series of absorption bands in the UV region that tail into the visible region. Probes **1** and **2** show fairly strong fluorescence with quantum yields of 0.022 and 0.26, respectively, in CH_3CN solution, determined by using diphenylanthracene in cyclohexane as the standard.[17] Probes **4** and **5** exhibit only very weak fluorescence with quantum yields less than 0.01. Probe **3** is nonemissive in air-equilibrated CH_3CN solution, possibly due to oxidative electron transfer from excited **3** to the LUMO of the nitro groups upon photoexcitation.

The ability of probes **1**–**5** to complex with anions was explored using UV/Vis absorption and fluorescence spectroscopy. Probe **1** displays colorimetric and fluorescent responses only to OH^-, F^-, and CN^- among the 11 anions (CN^-, F^-, Cl^-, Br^-, I^-, NO_3^-, OH^-, OAc^-, $H_2PO_4^-$, HSO_4^-, and ClO_4^-) tested. Addition of OH^-, F^-, or CN^- to probe **1** in CH_3CN resulted in solutions ranging from colorless to yellow. Figure 4 illustrates the changes in the absorption and fluorescence spectra of probe **1** in CH_3CN upon addition of CN^-. The absorption bands at 277 and 358 nm decreased while two new bands at 332 and 398 nm developed. Concomitantly, the fluorescence of **1** showed a bathochromic shift from 431 to 524 nm (ΔE_{em} = 4120 cm^{-1}).

Table 2. Photophysical properties of probes **1**–**5** in CH_3CN at 293 K.

Probe	Absorption	Fluorescence		
	λ_{max} [nm] (10^{-3} ε [$m^{-1}cm^{-1}$])	λ_{em} [nm]	Φ_{em}[a]	τ [ns]
1	277 (27.0), 358 (15.9)	431	0.022	<0.1[a]
2	292 (30.9), 380 (11.5)	428	0.26	0.89
3	276 (28.9), 358 (12.4)	[b]		
4	289 (43.1), 391 (6.0)	595	0.009	5.29
5	279 (38.3)	368	<0.0001	<0.1[a]

[a] The excited-state lifetime is too short for measurements with our instrument. [b] No detectable emission in solution at room temperature.

Probe **2** exhibited a strong response to CN^- and somewhat weak responses to OH^-, OAc^-, and $H_2PO_4^-$ in CH_3CN solution: The absorption bands at 292 and 380 nm decreased, while two new bands at around 302 and 440 nm developed and the fluorescence maximum of **2** showed a bathochromic shift from 428 to around 540 nm (ΔE_{em} = 4850 cm^{-1}). On the other hand, fluoride affected a more complicated response. Figure 5 shows the UV/Vis absorption spectra recorded in the course of the titration of probe **2** with F^-. Inspection of Figure 5(b) reveals that addition of

 © 2007 Wiley-VCH Verlag GmbH & Co. KGaA, Weinheim

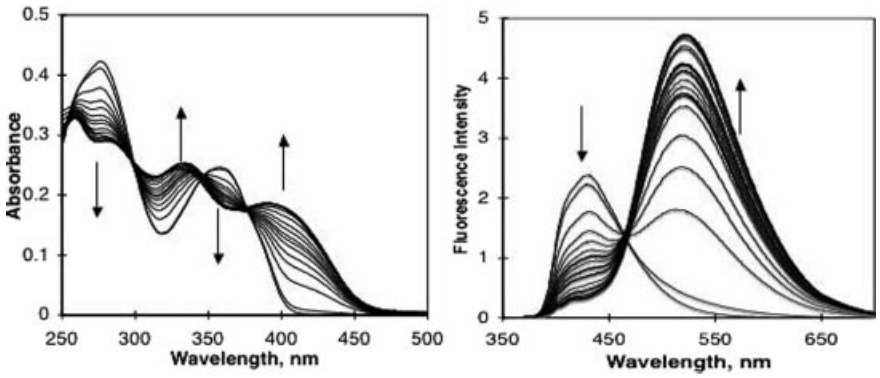

Figure 4. Changes observed in the absorption (left) and fluorescence (right) spectra of **1** (20 μM) upon addition of CN^- (0–6.0×10^{-4} M) in CH_3CN solution. Excitation was at 343 nm.

less than 1 equiv. of F^- to probe **2** resulted in a bathochromic shift of absorption bands from 292 and 380 nm to 296 and 390 nm, respectively, which is attributed to the formation of hydrogen-bonding interactions between the amide and pyrrole N–Hs with F^-, as inferred from ^1H NMR titration experiments. After addition of more than 1 equiv. of F^-, the deprotonation of the probe **2** is clearly signaled by the development of a new band at 450 nm and the color turned to yellow [see Figure 5(c)]. The fluorescence of **2** also displayed a bathochromic shift from 428 to 558 nm (ΔE_{em} = 5440 cm^{-1}). The concentration distributions, illustrated in Figure 5(d), of the three color species involved, **2**, **2**···F^-, and [**2**–H]$^-$, can be obtained by spectral deconvolution over the entire wavelength range using a nonlinear least-squares-fit algorithm, as implemented in the SPECFIT software package.[18]

Addition of CN^-, OH^-, F^-, OAc^-, and $H_2PO_4^-$ to probe **3** produced a color change from colorless to orange-red. Except for F^-, which apparently displays multiple equilibria in solution, a new band developed at around 480 nm on addition of CN^-, OH^-, OAc^-, or $H_2PO_4^-$. The UV/Vis spectroscopic titration profile of CN^- with probe **3** is illustrated in Figure 6. The newly developed absorption band of probe **3** at 470 nm reaches a maximum on addition of 2 equiv. of CN^-. Figure 7 shows the UV/Vis absorption spectra recorded in the course of the titration of probe **3** with F^- in

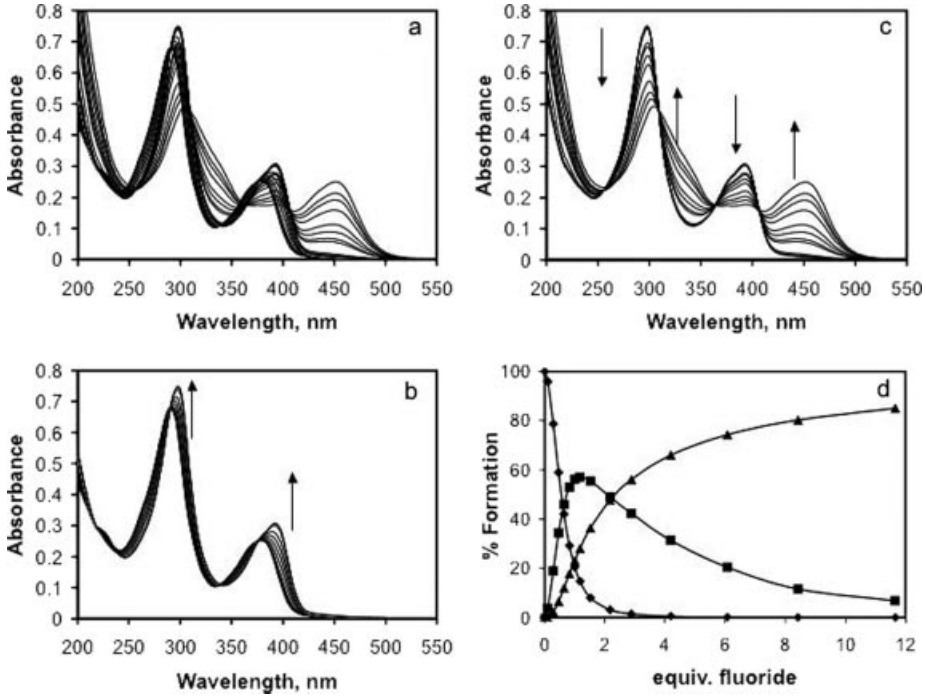

Figure 5. Spectrophotometric titration of probe **2** (1.4×10^{-5} M) with Bu_4NF in CH_3CN solution. (a) [F^-] = 0–1.6×10^{-4} M; (b) [F^-] = 0–1.6×10^{-5} M; (c) [F^-] = 1.6×10^{-5}–1.6×10^{-4} M; (d) % formation vs. equiv. of F^-; diamonds: probe **2**; squares: hydrogen-bonding complex [**2**·F^-]; triangles: deprotonated probe **2**, [**2**–H]$^-$.

 © 2007 Wiley-VCH Verlag GmbH & Co. KGaA, Weinheim

CH_3CN solution. A slight redshift in the absorption spectra was observed on addition of less than 1 equiv. of F^-. The absorption bands further bathochromically shifted to 318 and 490 nm in the presence of more than 1 equiv. of F^-.

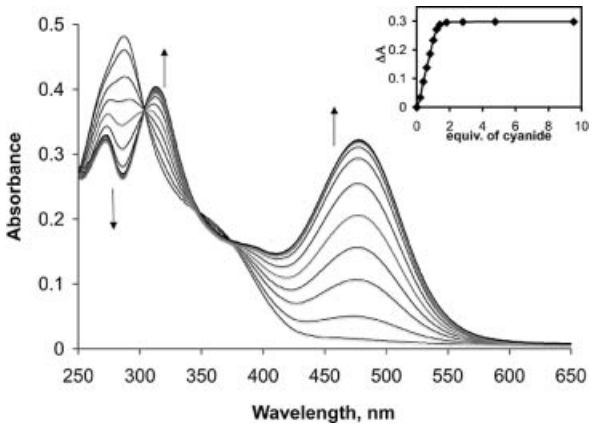

Figure 6. Changes in the absorption spectra of probe **3** (1.6×10^{-5} M) upon addition of CN^- in CH_3CN solution. The inset shows the absorbance changes at 470 nm as a function of equiv. of CN^-.

The titration isotherm clearly suggests the presence of two distinct processes in solution.

The spectrophotometric titrations of probes **4** and **5** with anions were carried out in DMSO solution because of the solubility issue. Probes **4** and **5** responded only to OH^-, CN^-, F^-, and OAc^- to produce a color change from red to purple for probe **4** and colorless to pale yellow for probe **5** in DMSO solution. Upon addition of these anions, the band at around 290 nm progressively decreased and the bands at around 390 and 550 nm developed for probe **4**, while the band at around 280 nm and shoulder at around 300 nm decreased and a new band at around 340 nm formed for probe **5**.

The equilibrium constants were determined by a spectral fitting procedure using a nonlinear least-squares-fit algorithm, as implemented in the SPECFIT program.[18] The results obtained from these analyses are collected in Table 3. In general, the equilibrium constants obtained from the spectrophotometric titrations are correlated to the basicity of the anions and the intuitive acidity of the amide and pyrrole N–H groups. In the case of probe **5** and F^-, attempts to derive the equilibrium constants by spectral fit-

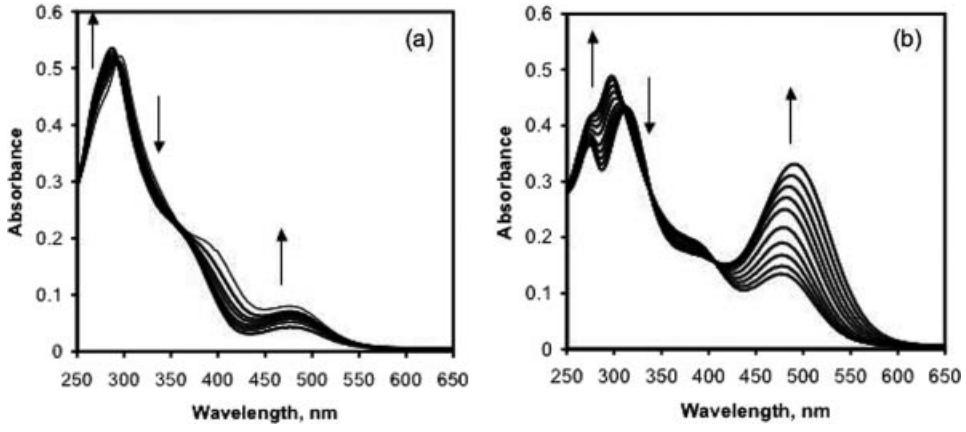

Figure 7. Changes in the absorption spectra of probe **3** (1.8×10^{-5} M) upon addition of F^- in the range (a) 0–1.7×10^{-5} M and (b) 2.5×10^{-5}–2.1×10^{-4} M in CH_3CN solution.

Table 3. Equilibrium constants [M^{-1}] for probes **1**–**5** in CH_3CN[a] or DMSO[b] solution at 20 °C, as determined by absorption spectroscopy titrations.[c]

Anion	Equilibrium constant K[d]				
	Probe **1**	Probe **2**	Probe **3**[e]	Probe **4**	Probe **5**
F^-	$K_a = 5.8\times10^3$	$K_a = 1.2\times10^4$ $K_d = 4.5\times10^7$	$K_a = 6.4\times10^4$ $K_d = 1.2\times10^7$	$K_a = 4.7\times10^3$ $K_d = 6.4\times10^4$	[f]
Cl^-	$K_a = 90$	$K_a = 110$	$K_a = 60$	$K_a = 110$	$K_a = 20$
OAc^-	$K_a = 190$	$K_d = 8.2\times10^5$	$K_d = 1.1\times10^6$ $K_a = 1.7\times10^3$	$K_a = 4.7\times10^4$	$K_a = 4.4\times10^4$
$H_2PO_4^-$	$K_a = 270$	$K_a = 2.3\times10^4$	$K_a = 7.7\times10^3$	$K_a = 250$	$K_a = 3.3\times10^3$
CN^-	$K_d = 1.9\times10^4$	$K_c > 1.0\times10^8$[e]	$K_c > 1.0\times10^8$[e]	$K_d = 4.8\times10^4$	$K_d = 1.8\times10^6$
OH^-	$K_a = 9.9\times10^4$ $K_d = 3.2\times10^5$	$K_d = 7.2\times10^5$	$K_d = 1.1\times10^6$	$K_d = 1.2\times10^4$	$K_d = 4.8\times10^4$

[a] For probes **1**–**3**. [b] For probes **4** and **5**. [c] The anions were added as tetrabutylammonium salts. [d] K_a, K_d, and K_c represent the association constant of the anion–probe hydrogen-bonded complex, the proton dissociation constant of the probe molecule, and the formation constant of the cyanohydrin complex, respectively. [e] A 1:2 probe/CN^- binding stoichiometry was found. The equilibrium constants cannot be precisely obtained due to steep titration isotherms. [f] The equilibrium constants did not satisfactorily fit the simple hydrogen-bonding or deprotonation processes.

 © 2007 Wiley-VCH Verlag GmbH & Co. KGaA, Weinheim

ting to hydrogen-bonding and deprotonation processes were unsuccessful. The possibility of the coexistence of different fluoride/probe **5** stoichiometries or the existence of subsequent reactions may contribute to the complexity of the solution equilibrium in this case.

Solvent polarity also influences the colorimetric response to the anion–probe interaction. High-polarity solvents tend to stabilize and favor the deprotonated species during the anion–probe interaction.[7b] Table 4 compares the absorption bands of probe molecules in DMSO, CH_3CN, and 1,2-dichloroethane (1,2-ClC_2H_4Cl) in the presence of 10 equiv. of F^-. An inspection of Table 4 reveals that the lowest-energy band is shifted to a longer wavelength in more polar DMSO than in less polar CH_3CN or 1,2-ClC_2H_4Cl, which suggests the large dipole presented in the anion–probe complex. The origin of the dramatic color changes observed in the presence of anion-induced neat proton transfer or nucleophilic cyanide addition might be ascribed to a charge-transfer process from the electron-rich deprotonated amide or cyanohydrin moiety to electron-deficient chromophoric units.

Table 4. Lowest-energy absorption bands obtained from the species derived from the interaction between F^- and probes **1**–**5** in different solvents.

Solvent	λ [nm]				
	1	**2**	**3**	**4**	**5**
1,2-$Cl_2C_2H_4$	362	396	[a]	[a]	304
CH_3CN	398	450	490	540	302
DMSO	413	462	500	548	343

[a] The data were not taken due to the insolubility in 1,2-dichloroethane.

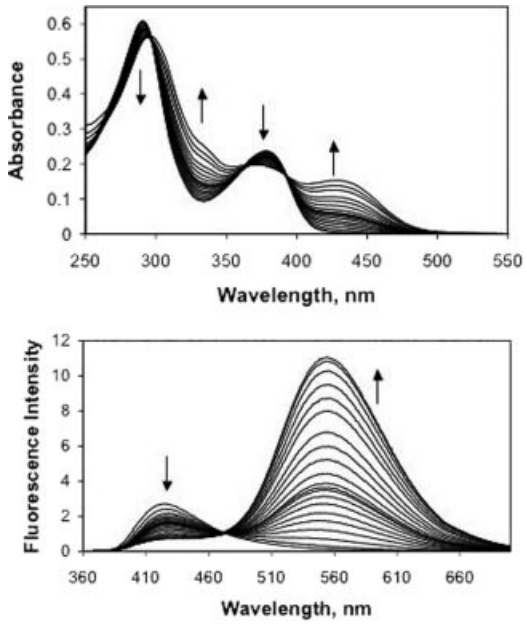

Figure 8. Changes observed in the absorption (top) and fluorescence (bottom) spectra of probe **2** (10 μM) upon addition of CN^- (0–5.2×10^{-4} M) in CH_3CN/H_2O (9:1, v/v) solution. Excitation is at 363 nm.

Colorimetric and Fluorescence Anion-Sensing in CH_3CN/H_2O (90:10, v/v) Solution

Except for probes **2** and **3**, for which the colorimetric and ratiometric fluorescent responses to CN^- persist, the colorimetric and ratiometric fluorescent responses of all the probes to the anions in the presence of water in CH_3CN or DMSO solution vanished. Figure 8 shows the changes observed in the absorption and fluorescence spectra of probe **2** upon addition of CN^- in CH_3CN/H_2O (90:10, v/v) solution. The absorption spectra display a bathochromic shift and the fluorescence bands are also redshifted from 425 to 554 nm. Similar absorption spectral changes were observed during the course of the titration of CN^- with probe **3** in CH_3CN/H_2O (90:10, v/v) solution. The association constants obtained by spectral-fitting for probes **2** and **3** are 1.1×10^9 and 7.9×10^5 M^{-2}, respectively.

Semi-Empirical ZINDO Calculations

The origin of the spectral transitions of the parent probe molecule and various types of anion–probe complexes was investigated by semi-empirical calculations using the ZINDO method implemented in the CAChe program.[19] Probe **3** was selected to demonstrate the variation of the HOMO and LUMO orbitals upon interacting with certain anions. The solvent-dependent absorption spectra of anion–probe complexes suggest a charge-transfer nature of the corresponding optical transitions. Figure 9 shows the HOMO and LUMO orbitals of parent probe **3**, the cyanohydrin form of probe **3**, and the amide N–H deprotonated probe **3**. It can be observed that the electron density of the LUMO orbitals of all three species is essentially located on the nitro groups but with a higher electron-density distribution in the cyanohydrin and the deprotonated forms of **3** than parent **3**, whereas the electron-density distribution of the HOMO orbitals is quite different. In the parent probe **3**, the HOMO is mainly delocalized on the pyrrole moiety. Upon deprotonation of the amide N–H group, the electron density of the HOMO orbital is delocalized from the amide nitrogen atom towards the phenyl ring and be-

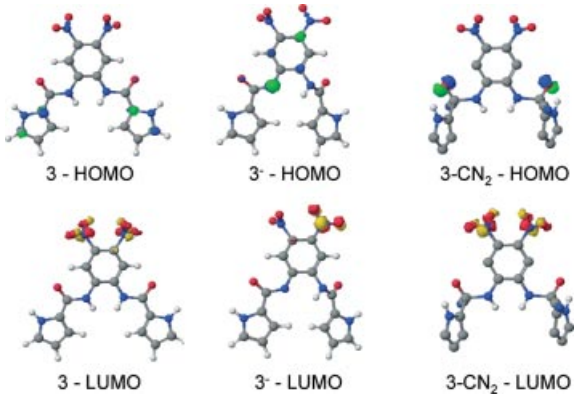

Figure 9. HOMO and LUMO orbitals of the parent, deprotonated, and cyanohydrin forms of probe **3**.

 © 2007 Wiley-VCH Verlag GmbH & Co. KGaA, Weinheim

comes a quinoid form of nitrobenzene. In the case of the cyanide adduct of probe **3**, the electron density of the HOMO orbital is essentially centered on the cyanohydrin oxygen atom. Both the cyanohydrin and deprotonated forms of **3** indeed exhibit the charge-transfer nature of the optical transition which accounts for the bathochromic shift observed in the absorption spectra.

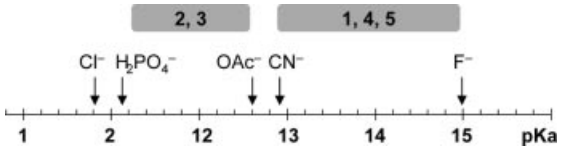

Scheme 5. Tentative acidic scale of the probe molecules in DMSO solution.

Discussion

The structures of probes **1**–**5** feature a pyrrolecarboxamide receptor moiety for anion-recognition and a chromogenic and/or fluorogenic unit for signal output after the anion interaction. We have found the hydrogen-bonding donating ability or acidity of N–H protons in this series of probes is directly related to the electron-withdrawing ability of the substituents on the chromogenic and/or fluorogenic unit and decreases in the order **3** > **2** > **5** > **4** ≈ **1**. Based on ^{1}H NMR titration experiments, the anion–probe interaction can be broadly classified into four different modes: weak hydrogen bonding, strong hydrogen bonding, acidic N–H deprotonation, and electron-deficient amide carbonyl addition. These different anion-interaction modes are primarily determined by both the anion basicity and N–H acidity. Chloride and dihydrogen phosphate are the two anions with the weakest basicity in our studies and, therefore, only a hydrogen-bonding interaction was observed in the ^{1}H NMR titration experiments. A slightly stronger basicity than Cl^- and its tetrahedral shape enable $H_2PO_4^-$ to form four hydrogen bonds with both of the amide and pyrrole N–H groups, while the spherical shape of Cl^- can only form two hydrogen bonds with the amide N–H groups. Multiple equilibria occurring in solution between the anion and probe molecule have been observed in several cases, including probes **1**–**5** with fluoride, probe **1** with hydroxide, and probe **3** with acetate and dihydrogen phosphate. In most situations, the typical behavior in the formation of multiple equilibria is the formation of a hydrogen-bonding interaction followed by neat proton transfer from the acidic amide N–H group to the anion. In the case of the addition of acetate to probe **2** in solution, neat proton transfer from an amide N–H group to the acetate indeed occurs before hydrogen-bond formation between the acetate and pyrrole N–H groups because of the highly electron-deficient nature of the amide N–H groups in probe **2**. With the information provided by the ^{1}H NMR titration experiments, the acidity scale of the amide N–H groups in probes **1**–**5** can be qualitatively estimated based on the observation of neat proton transfer during the titrations. Scheme 5 illustrates the relative pK_a values of the probes in DMSO solution.

The changes in the absorption and fluorescence spectra of all five probes on addition of anions are consistent with the observations in the ^{1}H NMR titration experiments. The formation of hydrogen-bonding complexes apparently exerts very little electronic perturbation on the electron-density distribution and, thus, the absorption and fluorescence spectra show almost no or very minor changes compared with the parent spectra. Therefore, the evidence for hydrogen bonding can only be inferred from the ^{1}H NMR experiments. On the other hand, observations of a noticeable bathochromic band shift in both absorption and fluorescence spectra generally imply that neat proton transfer occurs from the acidic amide N–H group to the anion. Semi-empirical ZINDO calculations confirm the charge-transfer nature of the lowest-energy optical transition in the anion-induced deprotonated probes. On the basis of the interaction modes between the anion and probe molecules inferred from the ^{1}H NMR and optical titration experiments, we were able to derive the equilibrium constants from the UV/Vis titration traces by spectral fitting procedures. The magnitudes of the equilibrium constants are also generally consistent with the order derived from the ^{1}H NMR titration experiments.

Cyanide represents a special case in our study. Unlike other anions we have investigated here, one chemical characteristic of cyanide is that it is a nucleophilic anion. Instead of simply forming hydrogen bonds with the amide N–H group or causing deprotonation of the acidic N–H group in the cases of probes **1**, **4**, and **5**, addition of cyanide resulted in nucleophilic addition on the electron-deficient amide carbonyl group in probes **2** and **3**. The potential hydrogen-bonding pocket, defined by the amide and pyrrole protons, tends to bring the cyanide into the vicinity of the amide carbonyl groups, and this, along with the strong electron-withdrawing nature of the NO_2 or quinoxaline functionality, renders the amide groups highly electron-deficient and susceptible to the nucleophilic addition by cyanide on the carbonyl groups. In particular, the ability of probes **2** and **3** to form covalently bonded complexes with cyanide

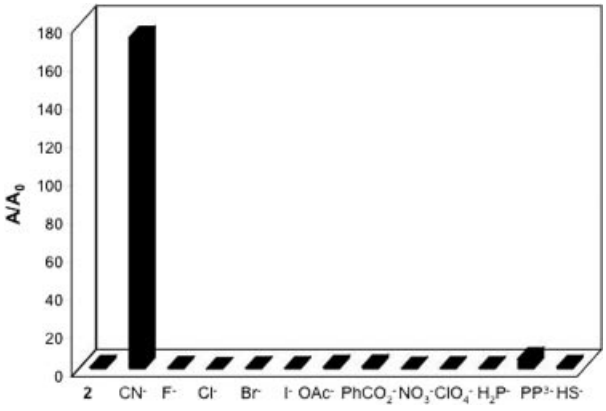

Figure 10. Absorbance response at 454 nm (A/A_0) of probe **3** (18 μM) in the presence of 10 equiv. of selected anions in CH_3CN/H_2O (1:1, v/v) solution.

 © 2007 Wiley-VCH Verlag GmbH & Co. KGaA, Weinheim

permits cyanide detection in semi-aqueous solution. The selectivity of CN^- over other anions, in particular fluoride, is important because most of the chemosensors reported for cyanide-sensing suffer the deleterious interference of other anions.[20] While a number of reports for selective cyanide-sensing have appeared in the literature,[21] only a few have demonstrated the potential to operate in competitive media.[22] The selectivity of probes **2** and **3** towards cyanide is vastly superior to other common anions, as can be seen from the absorbance response of probe **3** in the presence of various anions (see Figure 10).

Conclusions

A series of molecular probes integrating two pyrrolecarboxamide functionalities for anion-recognition and -sensing have been designed and synthesized. Anion-binding studies were carried out in CH_3CN, DMSO, or CH_3CN/H_2O solution. The nature of individual probe–anion interactions has been unambiguously defined by a combination of spectroscopic techniques including ^1H NMR spectroscopy, UV/Vis absorption, and fluorescence spectroscopy. Depending on the basicity and nucleophilicity of the anions as well as the electron deficiency of the acidic pyrrolecarboxamide N–H protons in the probe molecules, a variety of receptor–anion interaction modes could exist, namely, weak hydrogen bonding, strong hydrogen bonding, acidic N–H deprotonation, and electron-deficient amide carbonyl addition. Most importantly, the successful demonstration of ratiometric cyanide-sensing by probes **2** and **3** in a competitive medium (e.g. water) has paved the way to possible analytical applications. In light of the critical demand for a highly selective cyanide sensor, we believe the facile synthesis and modification of the structural framework of our chemosensors represents a new direction in the construction of functional chemical-sensing systems

Experimental Section

Materials and General Procedures: The starting materials, **7**,[23] **8**,[14] **9**,[24] and **13**,[25] were synthesized according to published methods. All other chemical reagents were commercially available and used without further purification unless otherwise noted. NMR spectra were recorded with either a Bruker AMX400 (400.168 MHz for ^1H and 100.622 MHz for ^{13}C) or a Bruker AV500 (499.773 MHz for ^1H and 125.669 MHz for ^{13}C) instrument. ^1H and ^{13}C chemical shifts are reported in ppm downfield from tetramethylsilane (TMS, δ scale) with the solvent resonances as internal standards. Absorption spectra were obtained using a Perkin-Elmer Lambda 900 UV/Vis/NIR spectrophotometer. Emission spectra were recorded in air-equilibrated CH_3CN solution at 298 K with a Fluorolog III photoluminescence spectrophotometer. Luminescence quantum yields were calculated relative to 9,10-diphenylanthracene in cyclohexane solution ($\Phi_{em} = 0.90$).[17] Corrected emission spectra were used for the quantum yield measurements. Luminescence quantum yields were taken as the average of three separate determinations and were reproducible to within 10%. Fluorescence lifetimes were measured with an Edinburgh Instruments Mini-τ single-photon counting lifetime spectrometer. The samples were excited at 370 nm with a diode laser. Nonlinear least-squares fitting of the decay curves were performed with the Levenburg-Marquardt algorithm and implemented with the Edinburgh Instruments T900 software. The errors in the fitted lifetimes are estimated to be within 10%. Absorption and fluorescence titrations were performed using a 2.0 mL probe solution in CH_3CN, CH_3CN/H_2O (90:10, v/v), or DMSO titrated with a sample of the anions prepared with the same probe solution to ensure the concentration of probe molecule does not vary during the titration. Absorption and fluorescence spectra were recorded following each addition of anion. The equilibrium constants, K, were determined by fitting the whole series of spectra at 1 nm intervals using the software SPECFIT 3.0 from Spectrum Software Associates, which employs a global system with expanded factor analysis and Marquardt least-squares minimization to obtain globally optimized parameters.[18] ^1H NMR titration experiments were carried out in $[D_6]$DMSO solution at a 1–5 mM concentration of the probe molecules. Semi-empirical ZINDO calculations were carried out to estimate the electron density and positions of the HOMO and LUMO orbitals. The structures were first optimized by semi-empirical AM1 calculations. Subsequently, the difference between the electron affinity and ionization potential was calculated by employing ZINDO using the program package CAChe.[19]

General Procedure for Preparing Anion Probes 1–5: A mixture of 1*H*-pyrrole-2-carbonyl chloride (200 mg, 1.5 mmol) and diamine (0.64 mmol) in CH_2Cl_2 (40 mL) and Et_3N (2 mL) was stirred at room temp. under nitrogen for 24 h. Probe **1** precipitated as a microcrystalline solid, which was collected and washed with CH_2Cl_2 and dried in vacuo. In the cases of probes **2**–**5**, precipitation did not occur; the volatiles were removed under vacuum. The residue was washed with 2 M hydrochloric acid (20 mL), diethyl ether, and CH_2Cl_2. The solid was further purified by column chromatography eluting with ethyl acetate to afford pure product.

Probe 1: ^1H NMR (400 MHz, $[D_6]$DMSO, 25 °C): δ = 6.10 (s, 2 H), 6.90 (s, 2 H), 6.95 (s, 2 H), 7.09 (t, $^3J_{H,H}$ = 4.4 Hz, 2 H), 7.37 (d, $^3J_{H,H}$ = 2.8 Hz, 2 H), 7.56 (d, $^3J_{H,H}$ = 4.8 Hz, 2 H), 9.35 (s, 2 H), 11.60 (s, 2 H) ppm. ^{13}C NMR (100 MHz, $[D_6]$DMSO, 25 °C): δ = 109.4, 112.3, 123.0, 125.3, 127.2, 127.8, 130.2, 134.4, 160.3 ppm. HREIMS: calcd. 465.0514 $[M + H]^+$; found 465.0435. $C_{22}H_{16}N_4O_2S_3 \cdot 0.5H_2O$ (473.59): calcd. C 55.79, H 3.62, N 11.83; found C 55.64, H 3.65, N 11.58.

Probe 2: ^1H NMR (400 MHz, $[D_6]$acetone, 25 °C): δ = 6.22 (dd, $^3J_{H,H}$ = 5.2, $^4J_{H,H}$ = 2.9 Hz, 2 H), 7.03 (s, 2 H), 7.10 (s, 2 H), 7.29–7.51 (m, 10 H), 8.48 (s, 2 H), 9.96 (s, 2 H), 11.09 (s, 2 H) ppm. ^{13}C NMR (100 MHz, $[D_6]$acetone, 25 °C): δ = 109.8, 111.6, 122.4, 123.3, 126.0, 128.0, 128.6, 130.0, 134.4, 138.9, 139.7, 153.1, 160.2 ppm. HREIMS: calcd. 499.1882 $[M + H]^+$; found 499.1887. $C_{30}H_{22}N_6O_2 \cdot 0.5H_2O$ (507.54): calcd. C 70.99, H 4.57, N 16.56; found C 71.34, H 4.54, N 16.59.

Probe 3: ^1H NMR (400 MHz, $[D_6]$DMSO, 25 °C): δ = 6.20 (m, 2 H), 7.05 (s, 2 H), 7.03 (s, 2 H), 8.55 (s, 2 H), 10.2 (s, 2 H), 11.9 (s, 2 H) ppm. ^{13}C NMR (100 MHz, $[D_6]$DMSO, 25 °C): δ = 110.2, 113.7, 121.8, 124.8, 125.4, 135.0, 138.2, 159.9 ppm. HREIMS: calcd. 385.0897 $[M + H]^+$; found 385.0898. $C_{16}H_{12}N_6O_6$ (384.30): calcd. C 50.01, H 3.15, N 21.87; found C 49.79, H 3.32, N 21.59.

Probe 4: ^1H NMR (400 MHz, $[D_6]$DMSO, 25 °C): δ = 6.19 (s, 1 H), 6.30 (s, 1 H), 6.84 (s, 1 H), 7.03 (s, 1 H), 7.11 (s, 1 H), 7.17 (s, 1 H), 7.90–7.93 (m, 2 H), 8.17–8.19 (m, 2 H), 8.21 (d, $^3J_{H,H}$ = 8.4 Hz, 1 H), 8.42 (d, $^3J_{H,H}$ = 8.8 Hz, 1 H), 10.02 (s, 1 H), 11.03 (s, 1 H), 11.93 (s, 1 H), 12.05 (s, 1 H) ppm. ^{13}C NMR (100 MHz, $[D_6]$DMSO, 25 °C): δ = 99.5, 109.5, 109.8, 111.2, 112.9, 123.9, 124.1, 125.0, 125.2, 125.4, 126.3, 127.1, 129.0, 129.78, 129.84,

 © 2007 Wiley-VCH Verlag GmbH & Co. KGaA, Weinheim

132.2, 134.3, 134.4, 134.5, 138.6, 158.5, 160.2, 181.5, 184.8 ppm. HREIMS: calcd. 424.1172 $[M]^+$; found 424.1176. $C_{24}H_{16}N_4O_4 \cdot H_2O$ (442.42): calcd. C 65.15, H 4.10, N 12.66; found C 65.28, H 3.87, N, 12.37.

Probe 5: ^{1}H NMR (400 MHz, [D$_6$]DMSO, 25 °C): δ = 6.18 (s, 2 H), 6.96 (s, 2 H), 7.01 (s, 2 H), 7.91 (s, 2 H), 9.85 (s, 2 H), 11.87 (s, 2 H) ppm. ^{13}C NMR (100 MHz, [D$_6$]DMSO, 25 °C): δ = 109.4, 111.9, 123.5, 125.07, 126.1, 126.3, 130.8, 159.3 ppm. HREIMS: calcd. 362.0337 $[M]^+$; found 362.0341.

Supporting Information (see footnote on the first page of this article): Representative absorption and fluorescence titration spectra and ^{1}H NMR titration spectra.

Acknowledgments

We are grateful to the National Science Council of Taiwan (Grant nos. 94-2113-M-001-014 and 95-2113-M-001-033-MY2) and Academia Sinica for support of this research.

[1] a) R. Martínez-Máñez, F. Sancenón, *Chem. Rev.* **2003**, *103*, 4419–4476, and references cited therein; b) P. D. Beer, P. A. Gale, *Angew. Chem. Int. Ed.* **2001**, *40*, 486–516; c) V. Amendola, D. Esteban-Gómez, L. Fabbrizzi, M. Licchelli, *Acc. Chem. Res.* **2006**, *39*, 343–353.

[2] a) P. A. Gale, "Amide and urea based anion receptors" in *Encyclopedia of Supramolecular Chemistry*, Marcel Dekker, New York, **2004**, pp. 31–41; b) P. A. Gale, J. L. Sessler, S. Camiolo, "Pyrrole- and polypyrrole-based anion receptors" in *Encyclopedia of Supramolecular Chemistry*, Marcel Dekker, New York, **2004**, pp. 1176–1185.

[3] a) C. B. Black, B. Andrioletti, A. C. Try, C. Ruiperez, J. L. Sessler, *J. Am. Chem. Soc.* **1999**, *121*, 10438–10439; b) H. Miyaji, H.-K. Kim, E.-K. Sim, C.-K. Lee, W.-S. Cho, J. L. Sessler, C.-H. Lee, *J. Am. Chem. Soc.* **2005**, *127*, 12510–12512; c) R. Nishiyabu, P. Anzenbacher Jr, *Org. Lett.* **2006**, *8*, 359–362; d) P. Anzenbacher Jr, M. A. Palacios, K. Jursíková, M. Marauez, *Org. Lett.* **2005**, *7*, 5027–5030; e) C.-Y. Wu, M.-S. Chen, C.-A. Lin, S.-C. Lin, S.-S. Sun, *Chem. Eur. J.* **2006**, *12*, 2263–2269.

[4] a) S.-S. Sun, A. J. Lees, *Chem. Commun.* **2000**, 1687–1688; b) A. M. Costero, M. J. Banuls, M. J. Aurell, M. D. Ward, S. Argent, *Tetrahedron* **2004**, *60*, 9471–9478; c) S. K. Kim, J. H. Bok, R. A. Bartsch, J. Y. Lee, J. S. Kim, *Org. Lett.* **2005**, *7*, 4839–4842; d) P. A. Gale, *Chem. Commun.* **2005**, 3761–3772; e) B. Liu, H. Tian, *J. Mater. Chem.* **2005**, *15*, 2681–2686; f) S. J. Brooks, L. S. Evans, P. A. Gale, M. B. Hursthouse, M. E. Light, *Chem. Commun.* **2005**, 734–736; g) S. Camiolo, P. A. Gale, M. B. Hursthouse, M. E. Light, A. J. Shi, *Chem. Commun.* **2002**, 758–759; h) L. S. Evans, P. A. Gale, M. E. Light, R. Quesada, *Chem. Commun.* **2006**, 965–967.

[5] D. Curiel, A. Cowley, P. D. Beer, *Chem. Commun.* **2005**, 236–238.

[6] a) K. Chellappan, N. J. Singh, I.-C. Hwang, J. W. Lee, K. S. Kim, *Angew. Chem. Int. Ed.* **2005**, *44*, 2899–2903; b) W. W. H. Wong, M. S. Vickers, A. Cowley, R. L. Paul, P. D. Beer, *Org. Biomol. Chem.* **2005**, *3*, 4201–4208; c) V. K. Khatri, S. Upreti, P. S. Pandey, *Org. Lett.* **2006**, *8*, 1755–1758.

[7] a) C. R. Bondy, P. A. Gale, S. J. Loeb, *J. Am. Chem. Soc.* **2004**, *126*, 5030–5031; b) M. Boiocchi, L. D. Boca, D. Esteban-Gómez, L. Fabbrizzi, M. Licchelli, E. Monzani, *J. Am. Chem. Soc.* **2004**, *126*, 16507–16514; c) T. Gunnlaugsson, P. E. Kruger, P. Jensen, J. Tierney, H. D. P. Ali, G. M. Hussey, *J. Org. Chem.* **2005**, *70*, 10875–10878; d) D. Esteban-Gómez, L. Fabbrizzi, M. Licchelli, E. Monzani, *Org. Biomol. Chem.* **2005**, *3*, 1495–1500; e) D. R. Turner, M. J. Paterson, J. W. Steed, *J. Org. Chem.* **2006**, *71*, 1598–1608; f) Y. Wu, X. Peng, J. Fan, S. Gao, M. Tian, J. Zhao, S. Sun, *J. Org. Chem.* **2007**, *72*, 62–70.

[8] P. A. Gale, *Acc. Chem. Res.* **2006**, *39*, 465–475.

[9] a) M. Boiocchi, L. D. Boca, D. Esteban-Gómez, L. Fabbrizzi, M. Licchelli, E. Monzani, *Chem. Eur. J.* **2005**, *11*, 3097–3104; b) L. S. Evans, P. A. Gale, M. E. Light, R. Quesada, *Chem. Commun.* **2006**, 965–967.

[10] A. Ajayaghosh, P. Carol, S. Sreejith, *J. Am. Chem. Soc.* **2005**, *127*, 14962–14963.

[11] a) X. Peng, Y. Wu, J. Fan, M. Tian, K. Han, *J. Org. Chem.* **2005**, *70*, 10524–10531; b) Z. C. Wen, Y. B. Jiang, *Tetrahedron* **2004**, *60*, 11109–11115; c) Y. Kubo, M. Yamamoto, M. Ikeda, M. Takeuchi, S. Shinkai, S. Yamaguchi, K. Tamao, *Angew. Chem. Int. Ed.* **2003**, *42*, 2036–2040; d) B. Yann, J. C. Martin, P. David, S. Rachel, *Chem. Commun.* **2002**, 1930–1931; e) S. Nishizawa, Y. Kato, N. Teramae, *J. Am. Chem. Soc.* **1999**, *121*, 9463–9464.

[12] Z. Yin, Z. Li, A. Yu, J. He, J.-P. Cheng, *Tetrahedron Lett.* **2004**, *45*, 6803–6806.

[13] S. J. Brooks, P. R. Edwards, P. A. Gale, M. E. Light, *New J. Chem.* **2006**, *30*, 65–70.

[14] C.-L. Chen, Y.-S. Chen, C.-Y. Chen, S.-S. Sun, *Org. Lett.* **2006**, *8*, 5053–5056.

[15] M. Boiocchi, L. Del Boca, D. Esteban-Gómez, L. Fabbrizzi, M. Lucchelli, E. Monzani, *Chem. Eur. J.* **2005**, *11*, 3097–3104.

[16] a) I. G. Shenderovich, P. M. Tolstoy, N. S. Golubev, S. N. Smirnov, G. S. Denisov, H. H. Limbach, *J. Am. Chem. Soc.* **2003**, *125*, 11710–11720; b) S. O. Kang, D. Powell, V. W. Day, K. Bowman-James, *Angew. Chem. Int. Ed.* **2006**, *45*, 1921–1925.

[17] S. L. Murov, I. Carmichael, G. L. Hug, *Handbook of Photochemistry*, Marcel Dekker, New York, **1993**.

[18] a) *SPECFIT*, version 3.0, Spectra Software Associates, Claix, France, **2005**; b) H. Gampp, M. Maeder, C. J. Meyer, A. D. Zuberbühler, *Talanta* **1985**, *32*, 95–101; c) H. Gampp, M. Maeder, C. J. Meyer, A. D. Zuberbühler, *Talanta* **1986**, *33*, 943–951.

[19] CAChe 5.0 for Windows, Fujitsu Ltd., Japan, **2001**.

[20] a) R. Badugu, J. R. Lakowicz, C. D. Geddes, *J. Am. Chem. Soc.* **2005**, *127*, 3635–3641; b) S.-S. Sun, A. J. Lees, P. Y. Zavalij, *Inorg. Chem.* **2003**, *42*, 3445–3453; c) P. Anzenbacher Jr, D. S. Tyson, K. Jursiková, F. N. Castellano, *J. Am. Chem. Soc.* **2002**, *124*, 6232–6233; d) H. Miyaji, J. L. Sessler, *Angew. Chem. Int. Ed.* **2001**, *40*, 154–157.

[21] a) Y. M. Chung, B. Raman, D.-S. Kim, K. H. Ahn, *Chem. Commun.* **2006**, 186–188; b) M. Tomasulo, S. Sortino, A. J. P. White, F. M. Raymo, *J. Org. Chem.* **2006**, *71*, 744–753; c) M. Tomasolu, F. M. Raymo, *Org. Lett.* **2005**, *7*, 4633–4636; d) C.-F. Chow, M. H. W. Lam, W.-Y. Wong, *Inorg. Chem.* **2004**, *43*, 8387–8393; e) D. Felscher, M. Wulfmeyer, *J. Anal. Toxicol.* **1998**, *22*, 363–366; f) A. Ajayaghosh, *Acc. Chem. Res.* **2005**, *38*, 449–459.

[22] a) J. V. Ros-Lis, R. Martínez-Máñez, J. Soto, *Chem. Commun.* **2002**, 2248–2249; b) F. García, J. M. García, B. García-Acosta, R. Martínez-Máñez, F. Sancenón, J. Soto, *Chem. Commun.* **2005**, 2790–2792; c) R. Badugu, J. R. Lakowicz, C. D. Geddes, *Anal. Chim. Acta* **2004**, *522*, 9–17; d) R. Badugu, J. R. Lakowicz, C. D. Geddes, *Dyes Pigm.* **2005**, *64*, 49–55; e) Y. Chung, H. Lee, K. H. Ahn, *J. Org. Chem.* **2006**, *71*, 9470–9474; f) Y. K. Yang, J. Tae, *Org. Lett.* **2006**, *8*, 5721–5723.

[23] C. Kitamura, S. Tanaka, Y. Yamashita, *Chem. Mater.* **1996**, *8*, 570–578.

[24] a) R. M. Acheson, *J. Chem. Soc.* **1956**, 4731–4735; b) G. W. H. Cheeseman, *J. Chem. Soc.* **1962**, 1170–1176.

[25] R. J. Boatman, H. W. Whitlock, *J. Org. Chem.* **1976**, *41*, 3050–3051.

Received: April 3, 2007
Published Online: June 28, 2007

 © 2007 Wiley-VCH Verlag GmbH & Co. KGaA, Weinheim